Specular reflection on Titan: Liquids in Kraken Mare

Katrin Stephan,[1] Ralf Jaumann,[1,2] Robert H. Brown,[3] Jason M. Soderblom,[3] Laurence A. Soderblom,[4] Jason W. Barnes,[5] Christophe Sotin,[6] Caitlin A. Griffith,[3] Randolph L. Kirk,[4] Kevin H. Baines,[6] Bonnie J. Buratti,[6] Roger N. Clark,[7] Dyer M. Lytle,[3] Robert M. Nelson,[6] and Phillip D. Nicholson[8]

Received 4 January 2010; revised 22 February 2010; accepted 25 February 2010; published 7 April 2010.

[1] After more than 50 close flybys of Titan by the Cassini spacecraft, it has become evident that features similar in morphology to terrestrial lakes and seas exist in Titan's polar regions. As Titan progresses into northern spring, the much more numerous and larger lakes and seas in the north-polar region suggested by Cassini RADAR data, are becoming directly illuminated for the first time since the arrival of the Cassini spacecraft. This allows the Cassini optical instruments to search for specular reflections to provide further confirmation that liquids are present in these evident lakes. On July 8, 2009 Cassini VIMS detected a specular reflection in the north-polar region of Titan associated with Kraken Mare, one of Titan's large, presumed seas, indicating the lake's surface is smooth and free of scatterers with respect to the wavelength of 5 μm, where VIMS detected the specular signal, strongly suggesting it is liquid. **Citation:** Stephan, K., et al. (2010), Specular reflection on Titan: Liquids in Kraken Mare, *Geophys. Res. Lett.*, *37*, L07104, doi:10.1029/2009GL042312.

1. Introduction

[2] Observations by the Cassini instruments revealed numerous large-scale dark surface features in Titan's polar regions [*Stofan et al.*, 2007; *Turtle et al.*, 2009]. Substantial evidence provided by the Cassini Radar instrument supports the interpretation that these regions are lakes consisting of liquid or solid hydrocarbons [*Stofan et al.*, 2007]. Nevertheless, liquids, mainly in form of ethane, have only been conclusively identified in Ontario Lacus, one of the few lakes in Titan's south-polar region [*Brown et al.*, 2008]. Detecting specular reflections of sunlight off of the lakes' surface by the optical Cassini instruments, however, which are sensitive in the visible and near-infrared spectral range, would also essentially eliminate anything but a body of liquid [*Williams and Gaidos*, 2008]. Until now, however, no specular reflections have been observed. The lack of observed specular reflections results either because the putative lakes are not filled with liquids or the lakes have not been observed in specular geometry. A further impediment is that the northern polar region, where several extensive features exists, including the more than 1000 km wide Kraken Mare [*Stofan et al.*, 2007; *Turtle et al.*, 2009], was not illuminated during Titan's long winter. Nevertheless, the northern polar region is now illuminated for the first time since Cassini arrived at Saturn in 2004, thus searches for specular reflections from northern bodies of liquid on Titan are now possible, with our first successful observations reported here.

2. Observations

[3] Three of four observations acquired by VIMS during the 58th flyby of Titan on July 8, 2009 (Table 1) show an unresolved feature with very high radiance seen only in the 5-μm atmospheric window (Figure 1). The feature is located near 71°N and 338°W. A quick review of the illumination and viewing geometry revealed that the bright spot occurred where the incidence and emission angles were about equal (~73°), which would be expected for a specular reflection of sunlight [*Shepard et al.*, 1993].

[4] We projected the VIMS observations accordingly to the geometry of the four VIMS cubes following the method of *Jaumann et al*. [2006]. In addition, Radar SAR images, used for comparison to the VIMS data, were processed as described by *Stephan et al*. [2009] following the methods of *Stiles et al*. [2008] that is based on the improved model of Titan's rotation, including the newly determined pole direction. Based on these data, the location of the specular reflection, with the size of the corresponding VIMS pixels of about 100 km across, can be associated with a Radar-dark region (Figure 2a). Although RADAR data do not cover this region completely and future data may reveal it as a separate lake, recent data imply that this region is part of the western edge of Kraken Mare [*Stofan et al.*, 2007; *Turtle et al.*, 2009].

[5] Figures 2b illustrates the predicted footprint of the solar disk derived from ray-tracing calculations, using position of the Sun, the spacecraft, and Titan (including the vector offset determined by the radius of Titan) for each of the observations. The size of the solar image was determined by projecting the edge of the solar disk onto the surface of Titan in the specular geometry. The size of the solar image calculated for these observations is sub-pixel; the semi-major axes of the elliptical footprint of the solar disk are ~4.4 and 1.3 km perpendicular and parallel to the Sun-Titan-spacecraft (specular) plane, respectively.

[6] During our observations, the location of the specular point moved from east to west (2 h 41 min) as the spacecraft flew by Titan. The observed variations in the strength of the

[1]Institute of Planetary Research, DLR, Berlin, Germany.
[2]Department of Earth Sciences, Institute of Geosciences, Free University, Berlin, Germany.
[3]Lunar and Planetary Laboratory, University of Arizona, Tucson, Arizona, USA.
[4]U.S. Geological Survey, Flagstaff, Arizona, USA.
[5]Department of Physics, University of Idaho, Moscow, Idaho, USA.
[6]Jet Propulsion Laboratory, California Institute of Technology, Pasadena, California, USA.
[7]U.S. Geological Survey, Denver, Colorado, USA.
[8]Department of Astronomy, Cornell University, Ithaca, New York, USA.

0094-8276/10/2009GL042312

Table 1. Observation Parameters of the VIMS Cubes Acquired During the Sequence CLOUDMAP001[a]

VIMS Cube (Cube Name)	Observation Time/Integration Time (ms)	S/C-Titan Center Distance[km]/Pixel Ground Resolution (km/pixel)	Location of S/C and Sub-Solar Points (Lat/Lon)	Brightest Pixel(s) (Sample/Line)	Location of the Center of the Brightest Pixel(s) (Lat/Lon)	Location of the Calculated Specular Reflection (Lat/Lon)
1 (1625724038)	(05:18:51 – 05:25:31/160)	233370/112.3	34.32128.199–0.371/313.309	5/27	72.98/339.03	71.27/336.22
2 (1625724520)	(05:25:53 – 05:55:13/640)	230936/109.25	34.32/128.424–0.371/313.544	4/284/29	70.03/335.1970.82/328.11	71.26/336.49
3 (1625730355)	(07:04:08 – 07:15:18/160)	200 887/95	34.236/129.795–0.370/314.952	7/327/33	71.62/338.9372.34/332.26	71.31/338.22
4 (1625731073)	(07:16:06 – 07:59:26/640)	195880/90.4	34.218/130.027–0.370/315.187	6/33	74.13/335.41	71.33/338.52

[a]Flyby T58.

Figure 1. (a) Bright spot in the northern polar region at ~72°N/342°W as seen in VIMS cube #3 (false color) that is restricted to the VIMS channels at 5 μm in comparison to (b) the corresponding observations geometry at the bright spot the viewing conditions on July 8, 2009 and (c) the location of the bright spot and the S/C point indicated by the red and green dots, respectively.

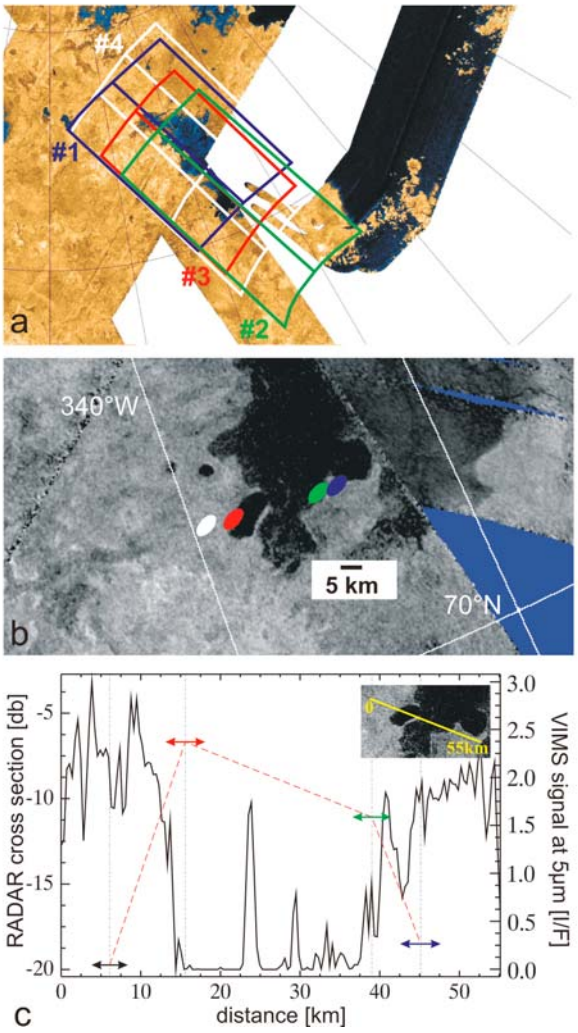

Figure 2. (a) Location and extension of the VIMS pixel that show a high reflectance at 5 μm (see Table 1) overlaid onto Radar SAR data (Titan flybys T19, T25, T28 and T29) implying a relation of the bright spot to Kraken Mare; (b) predicted positions of the Sun's reflection derived for the viewing conditions during the four VIMS observations; and (c) profile of the Radar signal (backscatter cross section) that goes through the locations of the four predicted solar reflections. Colored arrows indicate the positions of the solar reflections and the strength of the corresponding VIMS signal. The RADAR signal is scaled logarithmically to decibels (db) with −20 db equivalent to a Radar cross section ('sigma 0') value of 0.01.

5-μm signal in the individual VIMS spectra can be explained very well with the varying position of the Sun's footprint reflected from the surface. Only for VIMS cubes #2 and #3, where the 5-μm reflection is strongest, is the image of the Sun clearly associated with the lake itself, corroborated by the low Radar signal there (Figure 2c), and fulfilling the requirement of a specular reflection. VIMS pixel response function for point sources often results in illumination of two pixels when a point source is near a pixel boundary, explaining why the specular signal appears in two VIMS pixels as well. In contrast to VIMS cube #3, whose solar footprint (I/F = 2.84) lies almost entirely within the lake, the brightest pixels of VIMS cube #2 have a lower intensity (I/F = 2.1) because a fraction of the solar footprint possibly lies outside the lake. In that case, the observed intensity is lower, arising from a combination of the specular reflection off the lake and from light scattered by the adjacent terrain. In the case of VIMS cube #1, the image footprint is only partially within the lake explaining the weaker (I/F = 0.74), but still recognizable, 5-μm signal. The predicted position of the solar image for VIMS cube #4 of this observation sequence, whose spectrum shows only a weak signal at 5 μm (I/F = 0.57), is clearly located outside the lake.

3. Direct Versus Diffuse Flux of the Incidence Light Onto Titan's Surface

[7] The question arises as to why the specular reflections are seen only in the 5-μm window and not in the shorter-wavelength atmospheric transmission windows (Figure 3a). The detection of a specular reflection requires that a significant fraction of the incident sunlight is not scattered out of the beam, nor the light reflected from the surface be scattered during its travel out of the atmosphere. Within the atmospheric windows near 1.09, 1.6, 2, and 2.8 μm, less than 30% of the light is transmitted though the atmosphere for $i \sim 73°$, and less than 1/300 of this light traverses the atmosphere without being scattered (Figure 3b). Thus at wavelengths <3 μm, only a tiny fraction of the incident light traverses the atmosphere and reflects from the surface fully escaping any scattering event; specular reflection at these wavelengths is suppressed by atmospheric scattering. However, within the atmospheric window centered at 5 μm, the direct flux dominates and a significant fraction of the incident light reaching the surface has not been scattered [*Griffith et al.*, 2009]. Thus, we find that light specularly reflected from Titan's surface is exceptionally evident at 5 μm with a signal that is attenuated to roughly 15% (0.39 × 0.39 × 100%) by scattering and absorption by Titan's atmosphere.

4. Discussion of Surface Properties of Kraken Mare

[8] The observations strongly point to a specular reflection from a smooth surface, close to the southern shoreline of Kraken Mare. Only where the viewing geometry is such that the specular point falls onto one of the RADAR-dark surfaces do the VIMS observations show significant specular reflection. Thus, the most plausible explanation is a liquid surface that is smooth and free of scatterers with respect to the wavelength of 5 μm, where VIMS detected the signal. The observed intensity of the specular reflection is most consistent with reflection from a smooth body of liquid. We suggest that no plausible smooth solid surface could form naturally, nor if it did, remain smooth for very long in the presence of wind-driven erosion, settling of atmospheric haze particles, and saltation of surface particulates. Although CIRS data suggest the temperature on Titan's surface in the northern polar region (~90.5 K) is very close to the freezing point of both ethane and methane [*Jennings et al.*, 2009], a mixture of those compounds that will almost certainly contain some amount of nitrogen has a lower freezing temperature [*Barnes et al.*, 2009].

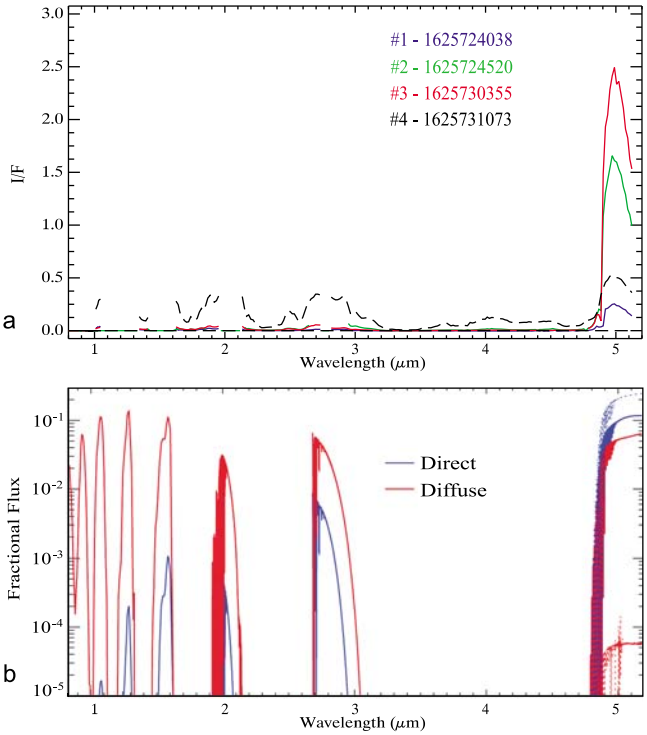

Figure 3. (a) VIMS spectra associated with the strongest reflection at 5 μm. Note that the spectrum of cube #4 (dotted line) that shows no specular signal were substracted from the spectra in order to isolate the specular signal in the spectra of the cubes #1 to #3. (b) Calculation of the diffuse (red) and direct (blue) flux that reaches Titan's surface for i = 73.64°. We use a discrete-ordinate, radiative-transfer model of *Griffith et al*. [2009]. The derivation assumes a plane parallel atmosphere, which, at this geometry, will not change the solution by more than ~50%. The haze characteristics are adopted from measurements by the Descent Imager/Spectral Radiometer (DISR) shortward of 1.6 μm, which are extended to 5 μm through fractal model fits to the data [*Tomasko et al.*, 2008a]. The methane opacity shortward of 1.6 μm is quantified from measured values by DISR, and longward of 1.6 μm from HITRAN line parameters [*Tomasko et al.*, 2008b; *Rothman et al.*, 2008], which were also used for the calculation of the carbon monoxide absorption. Shown at 5 μm are two atmospheric models: one is free of particulates (dotted lines) and one adopts the particulate distribution measured by Huygens at 10°S (solid lines). The vertical flux at the top of the atmosphere was set to 1, such that for the current lighting conditions a moon with a completely clear atmosphere would receive a relative flux of cos(73.64) = 0.282 at the surface.

[9] The expected intensity of the specular reflection when directly viewing the Sun in a reflection off a perfect, plane mirror at the distance of Titan (~1.26×10^7 for the VIMS IFOV) is reduced by: (1) the geometric defocusing of the flux by the convex reflecting surface; (2) the specular point being only partly filled by specular material; (3) the specular reflection falling between two VIMS pixels; (4) the finite, Fresnel reflectivity of the lake surface; and (5) the attenuation of the incoming and outgoing flux by the atmosphere. The effects of these factors on the maximum intensity of the specular reflection are explored in detail in a separate paper (J. M. Soderblom et al., manuscript in preparation, 2010). For the geometry described by the T58 flyby, the varying pixel-fill fraction, and assuming a refractive index of a surface consisting of liquid methane and/or ethane (~1.3), the Soderblom et al. model predicts a maximum I/F 1–3. This is consistent with the observed maximum intensity in the VIMS spectra at 5 μm, supporting the hypothesis that the specular signal observed by VIMS originates from a smooth, liquid surface.

[10] Our I/F value at 5 μm in cube #3, where the specular reflection is clearly associated with the lake itself, is close to the maximum of the modeled signal of a smooth liquid surface. Thus, we assume that no distinct amount of floating or suspended solid material with average particle sizes larger than 5 μm exists within the observed region of Kraken Mare, because it would significantly decrease or eliminate the specularly reflected signal. This is consistent with the findings of *Brown et al*. [2008], who rule out a significant fraction of >5-μm-sized solid material suspended in Ontario Lacus in order to explain their low signal at 5 μm, although they do argue for floating or suspended particles of 1–2 μm in size to explain their observation of a liquid ethane absorption at 2 μm.

[11] Macroscopic surface roughness also affects the measured intensity of the specular signal. *Cox and Munk* [1954] first studied this effect in Earth's oceans. The VIMS T58 specular observation is not spatially resolved. Hence a direct application of *Cox and Munk*'s [1954] technique will not work. However, because VIMS has four different measurements resolved in time, and if we assume that the surface properties do not change significantly along the track of the specular point, we can analyze the resulting lightcurve using forward-models in order to infer the surface normal distribution. The resulting best-fit parameters constrain the surface normal distribution in much the same way that spatially-unresolved lightcurves of transits can be used to characterize extrasolar planets [e.g., *Barnes and Fortney*, 2004]. Preliminary modeling (J. W. Barnes et al., manuscript in preparation, 2010) shows that the strong drop off in specularly reflected flux between observations #3 and #4 cannot be reproduced unless at least 94% of the sea surface slopes are less than 0.15°. The 3 mm constraint on the root-mean-square surface height variation on Ontario Lacus from the work of *Wye et al.* [2009] is essentially then the integral equivalent of our surface roughness constraint suggesting that like in Ontario Lacus not even capillary waves are present [*Lorenz et al.*, 2010] in the observed part of Kraken Mare. Conditions may change over larger distances, however, since Kraken Mare is a large sea. While no topographic information is available for the western part of Kraken Mare, Radar SAR images (Figure 2) give the impression of an 'upwind'-sheltered area with sharp, steep shoreline, in contrast to gradual mudflats seen on the margin of Ontario Lacus [*Brown et al.*, 2008; *Wye et al.*, 2009]. Future modelling of better-sampled specular lightcurves holds the promise for powerful constraints on shorelines, surface slopes, and spatio-temporal changes in wind-driven waves.

[12] **Acknowledgments.** We gratefully acknowledge the many years of work by the entire Cassini team that allowed these data of Titan to be obtained. We thank K.D. Matz for data processing support, R.D. Lorenz and an anonymous reviewer for valuable comments that significantly improved our manuscript. Part of this work was performed with support of DLR and the Helmholtz Alliance Planetary Evolution and Life.

References

Barnes, J. W., and J. J. Fortney (2004), Transit detectability of ring systems around extrasolar giant planets, *Astrophys. J.*, *616*, 1193–1203, doi:10.1086/425067.

Barnes, J. W., et al. (2009), Shoreline features of Titan's Ontario Lacus from Cassini/VIMS observations, *Icarus*, *201*, 217–225, doi:10.1016/j.icarus.2008.12.028.

Brown, R. H., L. A. Soderblom, J. M. Soderblom, R. N. Clark, R. Jaumann, J. W. Barnes, C. Sotin, B. Buratti, K. H. Baines, and P. D. Nicholson (2008), An ethane lake on Titan, *Nature*, *454*, 607–610, doi:10.1038/nature07100.

Cox, C., and W. Munk (1954), Measurement of the roughness of the sea surface from photographs of the Sun's glitter, *J. Opt. Soc. Am.*, *44*(11), 838–850, doi:10.1364/JOSA.44.000838.

Griffith, C. A., P. Penteado, S. Rodriguez, S. Le Mouelic, K. H. Baines, B. Buratti, R. Clark, P. Nicholson, R. Jaumann, and C. Sotin (2009), Characterization of clouds in Titan's tropical atmosphere, *Astrophys. J.*, *702*, L105–L109, doi:10.1088/0004-637X/702/2/L105.

Jaumann, R., et al. (2006), High-resolution CASSINI-VIMS mosaics of Titan and the icy Saturnian satellites, *Planet. Space Sci.*, *54*, 1146–1155, doi:10.1016/j.pss.2006.05.034.

Jennings, D. E., et al. (2009), Titan's surface brightness temperatures, *Astrophys. J.*, *691*, L103–L105, doi:10.1088/0004-637X/691/2/L103.

Lorenz, R. D., C. Newman, and J. I. Lunine (2010), Threshold of wave generation on Titan's lakes and seas: Effect of viscosity and implications for Cassini observations, *Icarus*, in press.

Rothman, L. S., F. J. Martin-Torres, and J.-M. Flaud (2008), Special issue on planetary atmospheres, *J. Quant. Spectrosc. Radiat. Transf.*, *109*, 881.

Shepard, M. K., R. E. Arvidson, and E. A. Guiness (1993), Specular Scattering on a Terrestrial Playa and Implications for Planetary Surface Studies, *J. Geophys. Res.*, *98*(E10), 18,707–18,718, doi:10.1029/93JE02089.

Stephan, K., et al. (2009), Mapping products of Titan's surface, in *Titan From Cassini-Huygens*, edited by R. H. Brown and M. Dougherty, pp. 489–510, Springer, New York.

Stiles, B., et al. (2008), Estimating Titan's spin state from Cassini SAR data, *Astron. J.*, *135*, 1669–1680, doi:10.1088/0004-6256/135/5/1669.

Stofan, E. R., et al. (2007), The lakes of Titan, *Nature*, *445*, 61–64, doi:10.1038/nature05438.

Tomasko, M. G., B. Bézard, L. Doose, S. Engel, E. Karkoschka, and S. Vinatier (2008a), Heat balance in Titan's atmosphere, *Planet. Space Sci.*, *56*, 648–659, doi:10.1016/j.pss.2007.10.012.

Tomasko, M. G., L. Doose, S. Engel, L. E. Dafoe, R. West, M. Lemmon, and E. Karkoschka (2008b), A model of the aerosols in Titan's atmosphere, *Planet. Space Sci.*, *56*, 669–707, doi:10.1016/j.pss.2007.11.019.

Turtle, E. P., J. E. Perry, A. S. McEwen, A. D. DelGenio, J. Barbara, R. A. West, D. D. Dawson, and C. C. Porco (2009), Cassini imaging of Titan's high-latitude lakes, clouds, and south-polar surface changes, *Geophys. Res. Lett.*, *36*, L02204, doi:10.1029/2008GL036186.

Williams, D., and E. Gaidos (2008), Detecting the glint of starlight on the oceans of distant planets, *Icarus*, *195*, 927–937, doi:10.1016/j.icarus.2008.01.002.

Wye, L. C., H. A. Zebker, and R. D. Lorenz (2009), Smoothness of Titan's Ontario Lacus: Constraints from Cassini RADAR specular reflection data, *Geophys. Res. Lett.*, *36*, L16201, doi:10.1029/2009GL039588.

K. H. Baines, B. J. Buratti, R. M. Nelson, and C. Sotin, Jet Propulsion Laboratory, California Institute of Technology, Pasadena, CA 91109, USA.

J. W. Barnes, Department of Physics, University of Idaho, Moscow, ID 83844-0903, USA.

R. H. Brown, C. A. Griffith, D. M. Lytle, and J. M. Soderblom, Lunar and Planetary Laboratory, University of Arizona, 1629 E. University Blvd., Tucson, AZ 85721, USA.

R. N. Clark, U.S. Geological Survey, Denver Federal Center, Mail Stop 964, Denver, CO 80225, USA.

R. Jaumann and K. Stephan, Institute of Planetary Research, DLR, Rutherfordstrasse 2, D-12489 Berlin, Germany. (katrin.stephan@dlr.de)

R. L. Kirk and L. A. Soderblom, U.S. Geological Survey, 2255 North Gemini Dr., Flagstaff, AZ 86011, USA.

P. D. Nicholson, Department of Astronomy, Cornell University, Ithaca, NY 14853, USA.